



CASE STUDY ON CAE TOOLS: OPTIMIZATION OF A 6-AXIS ROBOTIC ARM FOR MAG WELDING

Daniel Miler¹, Dragan Žeželj², Igor Lončarek³

Abstract: The design and optimization process of a 6-axis robotic arm for MAG welding is presented, with focus on the arm frame design. Different software tools are compared using the verification models for three types of analyses – dynamic, finite element static stress and fatigue stress analysis. After the appropriate tool was chosen for the task, simplified robotic arm models are made using the market analysis data. Dynamic analysis was conducted on said models and obtained results are used to dimension the initial model; which was then evaluated using the static stress and fatigue stress analysis. Process itself was iterative and above mentioned steps were repeated until the satisfactory results were achieved. Main advantage of this approach is the use of only one software interface and, since the focus is on the optimization, more energy efficient product.

Key words: Design, Fatigue stress, FEA, Optimization, Software verification

1 INTRODUCTION

With the development of industry, the need of productivity, reliability and the profitability also grew. Since man has limited motoric abilities, the need for productivity inspired new ideas. Solution was offered in 1954, when the first programmable industrial robotic arm patent was filed by Devol [1], indicating a change.

Today, serial industrial production is hard to imagine without the use of robots. Their tasks range from simple to the most complex ones. According to [2], one of the most dependent industry branches is the automotive industry; which accounted for almost 60% of the installed units in 2011. The surge in number of units sold causes product prices to fall and both the profitability and environment concerns to increase, which caused new design approaches to emerge. Environment and cost-effectiveness concerns largely inspired both the Design for Environment [3] and Design for Energy Minimization [4], new approaches that are growing in popularity. To keep both cost and environment impact low, early phases of the design process, where 90% of the cost and impact is generated [3, 5], should be addressed with special care.

¹ MSc, Daniel Miler, University of Zagreb, Zagreb, Croatia, daniel.miler@fsb.hr

² PhD, Dragan Žeželj, University of Zagreb, Zagreb, Croatia, dragan.zezelj@fsb.hr

³ MSc, Igor Lončarek, We-kr Ltd., Oberhausen, Germany, igor.loncarek@we-kr.com

In compliance with the above stated facts, the use of optimization tools on the design of a 6-axis robotic arm is presented, with the focus on the arm frame (detailing phase is omitted). Furthermore, computer aided engineering (CAE) tools are expensive and require time to master. In order to minimize number of different tools needed, software packs are evaluated using the verification models. After the verification, we assessed the possibility of using the only one CAE tool for the whole process.

2 SOFTWARE VERIFICATION

To determine the errors and applicability of each used software, verifications of the dynamic, static and the fatigue stress analyses were conducted. Since both the design [6] and optimization processes are iterative, the use of only one software (if possible) shortens the process. For various tasks, Solidworks, Autodesk Inventor, Ansys and MSC Adams results are compared. It is important to note that the main criterion for choosing the software was its applicability on a number of problems, and not necessarily the result exactness. Planned design process is shown on the Figure 1.

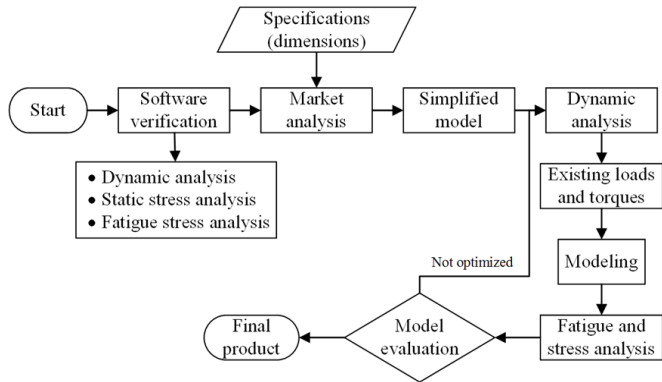


Figure 1. *Planned design process flowchart*

2.1 Dynamic analysis verification

MSC Adams (GSTIFF solver with I3 formulation was used) and Autodesk Inventor 2015 dynamic analyses results were compared. Dynamic analysis verification model consists of the lever rotating around the joint with constant rotational speed (Figure 2). During the rotation, reactional forces and torques appear in the joint. Calculated static torques are compared to the analytical solution (as shown in Table 1).

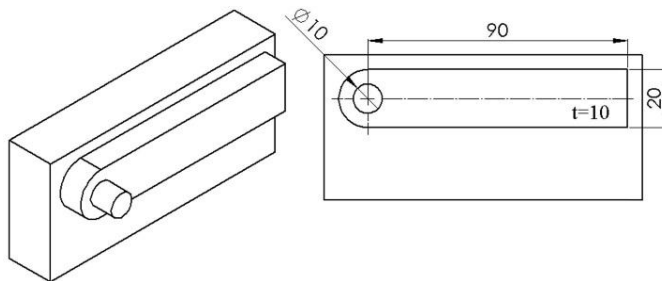


Figure 2. *Dynamic analysis verification model*

Table 1. *Torques and errors calculated on the verification model*

	Analytic	Inventor	Adams
Static torque M_{stat} / Nm	61.452	61.4773	61.4563
Error (%)	-	0.041	0.007

Since the error values are minimal, both the Autodesk Inventor and MSC Adams are considered validated.

2.2 Finite element stress analysis verification

For conducting the FEM stress analysis, Autodesk Inventor and Ansys are compared. Both are validated on the simple model for which analytical solution is known (Figure 3). Chosen specific load value is $q=0.05$ MPa. To ensure convergence, analysis is defined as adaptive, which enables the software to refine the mesh until the pre-defined criteria is met. Currently, two criteria exist [7]:

- Maximum number of h refinements – specifies the number of h refinement cycles for convergence. Its chosen value is 4, with default refinement threshold value $h=0.75$.
- Stop criteria – ceases the refinement when the difference between the two consecutive results is less then specified. Chosen value is 2%.

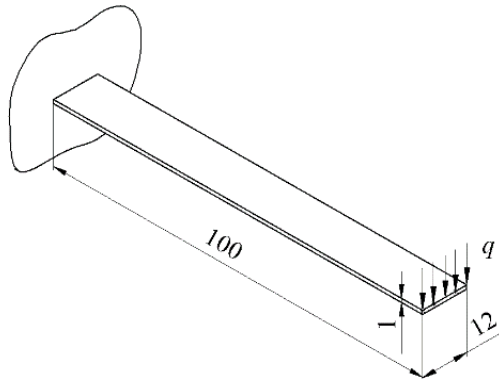


Figure 3. *Numeric stress analysis verification model*

Also, Inventor enables the use of linear and quadratic tetrahedral finite elements for 3D analysis; which were compared to the Ansys results for the quadratic tetrahedral and quadratic hexahedral elements. Results are shown in the Table 2.

Table 2. *Results of the FEM stress analyses*

Variable	Unit	Analytical	Autodesk Inventor		Ansys	
			Linear tetrahedral	Quadratic tetrahedral	Quadratic tetrahedral	Hexahedral
σ_{max}	MPa	30	29.01	30.413	29.646	29.616
E_{σ}	%	-	-3.41	1.348	-1.194	-1.297
w	mm	1	0.9857	0.9874	0.985	0.987
E_w	%	-	-1.451	-1.276	-1.527	-1.3182

2.3 Fatigue stress analysis verification

Due to fatigue, machine element fractures can be caused by stresses lower than the material tensile strength. According to ASM [8], fatigue accounts for 80% of all the cost associated with the fracture of metal structures. The ASME [9] example (stress history shown on Figure 4) was used for the software verification. It consists of the plate ($\delta \ll b, h$) under the uniform tensile stress of 1 MPa. Since the stress cycle amplitudes are variable, Rainflow method [10] was used to enable the use of the Palmgren-Miner rule.

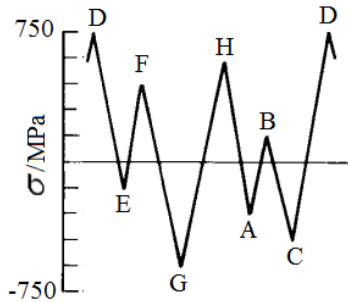


Figure 4. Resulting repeating cycle from ASME example

Table 3. Stress cycles after the use of Rainflow method

$\sigma_a /$ MPa	$\sigma_m /$ MPa	n	Flow path
675	75	1	D-G
525	75	1	H-C
300	150	1	E-F
225	-75	1	A-B

By using the Palmgren-Miner rule on the example above, number of cycles before the break was calculated. S-N curve equation (1) for S355 steel (material properties found in [11]) was used to calculate the said number without the influence of mean stress:

$$S_a = S'_f \cdot N_f^{b_f} \quad (1)$$

Impact of mean stress σ_m (Table 3) was determined using the Soderberg, Gerber and Goodman relations. Solidworks and Ansys were used for the numerical solutions.

Table 4. Fatigue stress analysis verification results

Relation	Analytical solution	Ansys		Solidworks	
		N_f	Error (%)	N_f	Error (%)
$N_f (-)$	45.063	45.066	0.0067	44.433	-1.418
N_f (Goodman)	8.669	8.6735	0.0519	8.554	-1.327
N_f (Gerber)	36.486	36.493	0.0192	35.984	-1.395
N_f (Soderberg)	2.3502	2.3504	0.0085	2.326	-1.0404

Both Ansys and Solidworks solution errors are low (Table 4), however Solidworks solution displays a greater error – by two orders of magnitude. Furthermore, after observing the Tables 1 and 2, Ansys-Inventor combination was chosen. Since Ansys can be integrated into the Autodesk Inventor, it's possible to complete all the analyses using only one software interface.

3 DESIGN PROCESS

Market analysis was undertaken in order to gather the design parameters needed to create the simplified model. The customer needs, competition products and current product design trends were considered. Following key features are identified: load capacity, maximal velocity, arm reach, repeatability and precision. Resulting desired specifications are shown in Table 5.

Table 5. Chosen design specifications

Manufacturer	Model	Capacity	Reach	Mass
Yaskawa Motoman	Motoman MA 1550	3 kg	1.584 m	130 kg
Asea Brown Boveri	IRB 1520 ID	4 kg	1.500 m	170 kg
Kuka	KR 16 arc HW	8 kg	1.636 m	245 kg
Fanuc	ARC Mate 100iC/7L	7 kg	1.632 m	135 kg
Chosen specifications		6 kg	1.800 m	-

Next step was designing the simplified model (Figure 5) for the dynamic analysis which was conducted using both MSC Adams multibody dynamics simulation software and Autodesk Inventor 2015. Analysis provided the load conditions arm has to withstand.

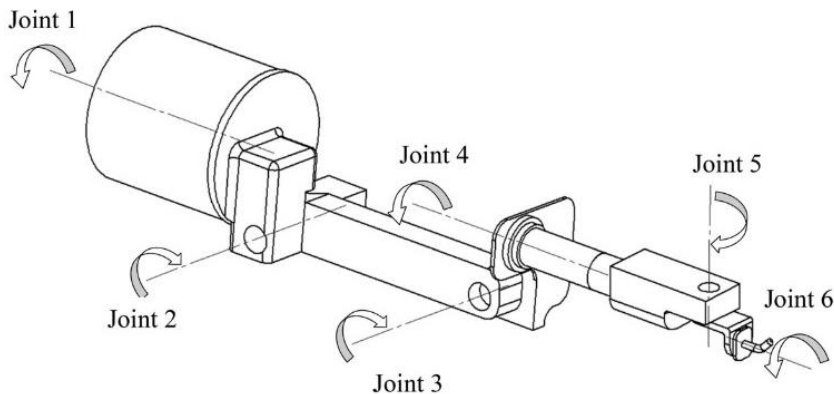


Figure 5. Simplified model

By using the simplified model and desired rotational accelerations and velocities, loads and torques that can be used for dimensioning are calculated. It is important to note that due to limited space only analyses of the critical parts will be shown in this article. Also, during the iteration process loads change due to the changes in the part geometries, so the dynamic analysis will be repeated in order for product to be optimized.

3.1 Finite element stress analysis

After the part is modelled, stresses are determined using the finite element static stress analysis. Parts are loaded according to the previously performed dynamic analysis, and mesh refinement was varied to ensure convergence. Only the analyses of the most heavily loaded parts are shown in this article (Figure 7). Qualitative deformations are also displayed (red – highest, blue no deformation).

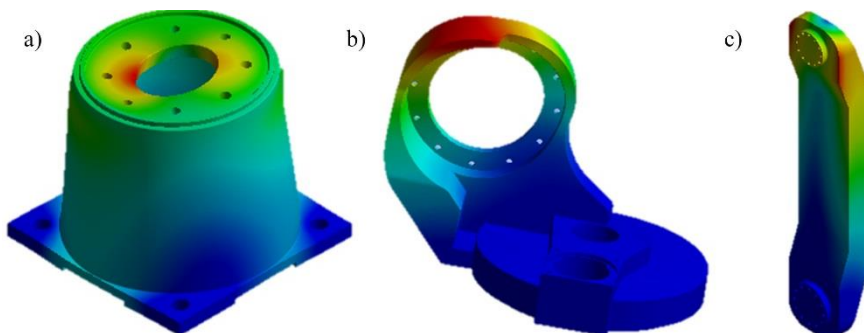
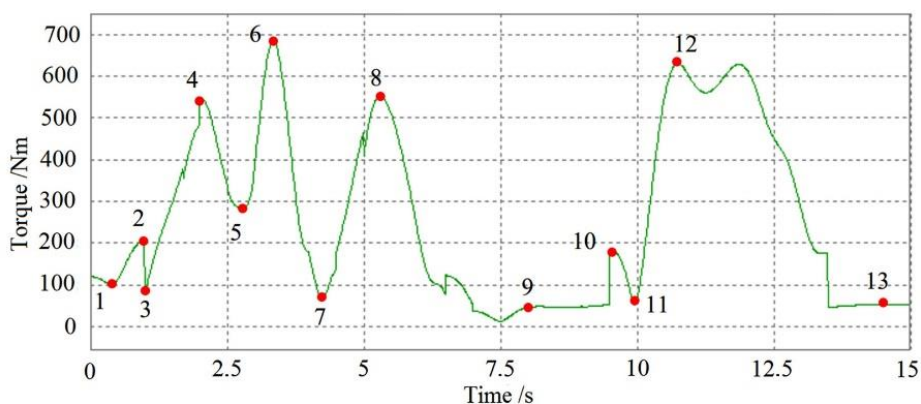


Figure 7. Arm parts; a) base, b) rotation stand and c) arm section 1

To simplify the numeric model, components of the robotic arm are constrained as *fixed support*. Since time difference between the largest torques on each of the axes is small, to remain on the side of safety regarding the stress, models are loaded as if torques appear simultaneously.

3.2 Fatigue stress analysis

In contrast to static analysis, where maximal loads were used regardless of the time, fatigue analysis considers both the time of occurrence and load magnitude. Since rotational plate displayed largest deformations and stresses during the static FEM analysis, it is chosen for a further analysis. Overall torque $T_{\Sigma}=T(t)$ is calculated (Figure 8). Torque peaks which will be used in the analysis are also shown.

Figure 8. Overall torque $T_{\Sigma}(t)$

Simplified analytical model was used to determine the load at the specified time. Only the highest load (in the each of the 13 points) has been observed, and was later used as the maximum stress of the fully reversed cycle and the repeated stress cycle with the mean stress influence calculated using Gerber formulation.

Based on Ansys results it could be determined that the number of cycles before the break is above the 10^9 cycles. Lastly, it should be noted that simplifications were used. In order to ensure safety, most adverse load conditions were used. In order to calculate the more precise number of cycles, elasticity of the components should be included in the analysis.

Table 6. Loads and principal strain calculated in the observed time points

	Load						Stress (Von Mises)
Point	F_x / N	F_y / N	F_z / N	M_x / Nm	M_y / Nm	M_z / Nm	σ_{eq} / MPa
1	12	-567	-73	77.69	4.79	60.01	12.52
2	-122	-575	-48	80.32	17.42	-194.02	18.1
3	68	-575	-45	72.91	26.58	10.52	11.43
4	-70	-700	355	36.07	-282.7	-465.08	53.25
5	-874	-710	281	79.91	-185.27	-200.69	27.72
6	-770	-540	-348	246.36	214.08	-600.34	68.04
7	-59	-544	-8	-14.12	2.2	-63.09	10.71
8	280	-593	169	-131.26	78.9	530.98	55.24
9	-13	-586	15	-9.84	3.73	46.82	6.59
10	110	-598	20	-1.51	1.96	183.23	16.43
11	90	-526	45	-34.08	-5.47	39.72	7.51
12	-379	-594	-169	80.03	174.84	-600.4	45.41
13	0	-586	0	3.16	0	52.19	7.44

4 RESULTS AND DISCUSSION

After the manual iteration process was finished (as stated in Figure 1), the resulting design (Figure 9) was detailed. Wanted specifications of the final product have been met (reach of 1.8 m and load capability of 6 kg). With decreasing the mass, energy costs also decrease, so the estimated mass of the assembly (131.5 kg) is considered its greatest advantage ahead of the competition (Table 5). Most of the parts are made of aluminium, with except of the steel base parts (greatest stress).



Figure 9. Final design

While decreasing the mass, special care should be devoted to the rigidity of the system. Even though the stresses values may be low, if left uncontrolled deformations may cause lower precision. Using one software interface has many benefits. During the manual optimization phase, parametric modelling enabled changing the dimensions directly in the FEA software, which proved to be time saving. Change was automatically linked to CAD model. Also, software integration offered easier modelling coupled with the FEA software robustness.

On the other hand, calculation error should also be addressed. As shown on the Table 1, dynamic analysis results using Autodesk Inventor show greater error. In [12] Bernd et al. found that while using different FEA tools on the same part, calculated stresses can dissipate up to 50%; meaning that even though the software integration is time saving, it can be contra-productive if the software operator lacks knowledge about the mathematical background. Furthermore, in order to carry out the described process, both software licences have to be purchased.

5 CONCLUSION

6-axis robotic arm for MAG welding has been designed and optimized. Also, the use of only one software interface (Autodesk Inventor with integrated Ansys) for both the modelling and analysing was validated; which decreases the time spent, cost, and reduces the error encountered while transferring the data between the different software.

During the design, many CAE tools were used in order to reach the optimal solution. In the future, the robotic arm can be further optimized by using the dynamic analysis with elastic components to provide more exact loads, deformations and accurate precision assessment. Also, the use of topology optimization could prove beneficial to the design.

REFERENCES

- [1] Devol, G. C., 1954, *Programmed article transfer*, United States of America Patent US2988237 A.
- [2] Statista Inc, 2015, *The Statistic Portal*, Statista Inc, [Online] <http://www.statista.com/topics/1476/industrial-robots/>. [Accessed June 13 2016].
- [3] Moultrie, J., Sutcliffe, L., Maier, A., 2016, *Exploratory study of the state of environmentally conscious design in the medical device industry*, Journal of Cleaner Production, vol. 122, pp. 252-265.
- [4] Seow, Y., Goffin, N., Rahimifard, S., Woolley, E., 2016, A 'Design for Energy Minimization' approach to reduce energy consumption during the manufacturing phase, Energy, vol. 109, pp. 894-905.
- [5] Roche, T., 2005, *The Design for Environmental Compliance Workbench Tool*, Product engineering: Eco-design, technologies and green energy, Dordrecht, Springer, 2005, pp. 9-17.
- [6] Dym, C. L., 2014, *Engineering Design: A Synthesis of Views*, Cambridge: Cambridge University Press
- [7] Autodesk, 2014, Convergence Settings, [Online] <https://knowledge.autodesk.com/support/inventor-products/learn-explore>. [Accessed June 15 2016].
- [8] Hudgins, A., James, B., 2014, *Fatigue of Threaded Fasteners*, Advanced Materials & Processes, no. august, pp. 18-22.
- [9] ASTM International, 2011, *ASTM E1049-85(2011)e1 Standard Practices for Cycle Counting in Fatigue Analysis*, West Conshohocken: ASTM International.
- [10] Matsuishi, M., Endo, T., 1968, *Fatigue of metals subject to varying stress*, Proc. Kyushu Branch of Japan Society of Mechanical Engineering, pp. 37-40.
- [11] De Jesus, A. M., Matos, R., Fontoura, B. F., Rebelo, C., Da Silva, L. S., Veljkovic, M., 2012, *A comparison of the fatigue behavior between S355 and S690 steel grades*, Journal of Constructional Steel Research, no. 79, pp. 140-150.
- [12] Roith, B., Troll, A., Rieg, F., 2007, *Integrated Finite Element Analysis (FEA) in Three-Dimensional Computer Aided Design Programs (CAD) - Overview and Comparison*, Proceedings of ICED 2007, the 17th international conference on engineering design, pp. 1-12., The Design Society.